Density Functional Theory Calculations of the Transition States for Hydrogen Exchange and Dehydrogenation of Methane by a Brønsted Zeolitic Proton

S. R. Blaszkowski,*,†,‡ A. P. J. Jansen,† M. A. C. Nascimento,‡ and R. A. van Santen†

Schuit Institute of Catalysis, Laboratory of Inorganic Chemistry and Catalysis/Theory Group, Eindhoven University of Technology, P. O. Box 513, 5600 MB Eindhoven, The Netherlands, and Instituto de Química, Departamento de Físico-Química, Universidade Federal do Rio de Janeiro, Ilha do Fundão, Cidade Universitária, CT, Bloco "A", Rio de Janeiro, RJ, 21949−900 Brazil

Received: July 5, 1994; In Final Form: September 22, 1994[⊗]

Density functional and semiempirical (MNDO) theories are used to determine transition states and the corresponding activation barriers of hydrogen exchange and dehydrogenation of methane catalyzed by a protonated zeolite cluster model. The nonlocal density functional activation barriers were found to be 125 and 343 kJ/mol for hydrogen exchange and dehydrogenation, respectively. From the imaginary frequency of one of the transition state eigenmodes, the reaction coordinates were deduced. Additionally, from the activation barrier and vibration, rotation, and translation partition functions, reaction rate constants have been evaluated using transition state reaction rate theory.

1. Introduction

As crystalline aluminosilicate framework structures, zeolites contain networks of channels and cavities capable of hosting a range of molecules and ions.[1] Acidic zeolites that contain Brønsted acidic sites catalyze a wide variety of chemical reactions. The catalytic properties of zeolites make them very valuable in a variety of industrial processes. In oil and petrochemical industries for example, zeolites are largely used for processes such as cracking, isomerization, and alkylations of hydrocarbons.[2] The mechanisms by which these reactions proceed involve proton transfer and formation of carbenium or carbonium ions as reactive intermediates.[3] The details of these processes are still little understood. The experiments[4] indicate that electrophilic activation of light alkanes occurs in superacid catalysts at low temperature and on weaker solid acids at higher temperatures, apparently via heterolytic cleavage of C−H bonds. However, the difference between the elevated working temperatures of zeolite catalysts and the moderate temperatures at which superacids are used should not be overlooked when comparing kinetic parameters of carbocation rearrangements in both systems.

A significant effort is being done in the field of understanding the relation between acidity and catalytic activity of zeolites.[5] The acidity function is due to protons that are attached to the oxygen atoms of the zeolite framework. Catalytic activity is, at least partially, related to the intrinsic acid strength of the protons. At present, a proper definition of acid strength for a solid acid is lacking, and its relation to catalytic activity is not well understood. Kramer et al.[6] proposed that the difference in proton affinity between neighboring oxygen atoms of the active site is of importance. In their paper over hydrogen/deuterium exchange of perdeuterated methane (CD_4) they explained the difference in reactivity of two different zeolitic structures, faujasite and MFI. The reaction barrier height is found to increase with increasing proton affinity difference between the two structurally neighboring oxygen atoms. This explains for this reaction the different activity of the two zeolites of the same composition.

Depending on the acidity properties of the catalyst and the sort of reaction involved, different carbocations can be formed.[3] Among the carbocations of concern for the conversion pathways of alkanes, a distinction has to be made between alkylcarbenium and alkylcarbonium ions. Alkylcarbenium ions contain a tricoordinated positively charged carbon atom, the three substituents being alkyl groups or hydrogen atoms. Alkylcarbonium ions contain a pentacoordinated positively charged carbon atom, having the same type of substituents. In the carbonium ions that will be encountered, at least one of the five substituents is a hydrogen atom.

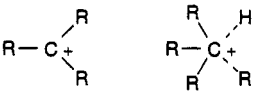

These carbocations can occur according to different mechanisms. The protonation of an alkene (olefin) by the acid zeolite (HZ) leads to the formation of an alkylcarbenium ion. If the proton is added to a saturated molecule such an alkane (paraffin), the protonation leads to the formation of an alkylcarbonium ion. The alkylcarbonium ion can also be transformed into a smaller alkylcarbenium ion by abstraction of an electroneutral molecule (an alkane or molecular hydrogen), involving explicitly cracking reactions. The activation of an alkane is more difficult than that of an alkene and occurs under high temperatures condition.

In order to better understand the intermediates involved in the reactions between hydrocarbons and an acidic zeolite, the carbonium and carbenium ions, this work proposes a detailed study of the transition states and kinetics involved in the reaction between methane and the zeolite. When methane is in contact with the acidic site of the zeolite, the reactions hydrogen/deuterium (eq 1a) or hydrogen/hydrogen exchange (eq 1b) and dehydrogenation (eq 2) can occur (‡ indicates transition state):

$$ZOH + CD_4 \rightarrow (ZO^- \cdots CD_4H^+)^{\ddagger} \rightarrow ZOD + CD_3H \quad (1a)$$

$$ZOH + CH_4 \rightarrow (ZO^- \cdots CH_5^+)^{\ddagger} \rightarrow ZOH + CH_4 \quad (1b)$$

$$ZOH + CH_4 \rightarrow (ZO^- \cdots CH_3^+ \cdots H_2)^{\ddagger} \rightarrow ZOCH_3 + H_2 \quad (2)$$

Hydrogen/deuterium exchange between alkanes and superacids is believed[7] to involve carbonium ions, under conditions in which cracking does not take place. Kramer et al.[6] propose for

† Eindhoven University of Technology.
‡ Universidade Federal do Rio de Janeiro.
⊗ Abstract published in *Advance ACS Abstracts,* November 1, 1994.

0022-3654/94/2098-12938$04.50/0

the reaction of hydrogen/deuterium exchange of methane a transition state with characteristics of a carbonium ion, where the carbon atom is symmetrically pentacoordinated to hydrogen atoms. The reaction temperatures used were between 600 and 750 K. Evleth et al.,[8] on the other hand, from a theoretical study for the same reaction propose a transition state with characteristics of methyl radical bound to H_2^+, ($CH_3-H_2^+$) due to a negative charge found in the methyl group. Mota et al.[9] have performed experiments on the hydrogen/deuterium exchange between zeolite Y and 3-methylpentane and methylcyclohexane. They propose that zeolites can protonate σ bonds of tertiary alkanes at 373 K without cracking, probably through an intermediate or transition state having a five-coordinated carbonium ion. This suggests initial formation of carbocations in alkane cracking. They propose that the migration of deuterium to primary and secondary carbons is stereochemically more favorable than that to a tertiary carbon. Here the transition state for reaction 1b is analyzed using density functional theory. The symmetric exchange between a proton of the zeolite and a hydrogen of the methane occurs via a transition state similar to a carbonium ion. A comparison with earlier results of Kramer et al.[6] and Evleth et al.[8] will be presented. The isotopic effect involving the perdeuterated methane in reaction 1a was not included, since it has been found to be not very significant at reaction temperatures.[10]

The catalytic conversion of methane to desired chemical products or liquid fuel is a great challenge to catalysis science. Wang et al.[11] studied the dehydrogenation and aromatization of methane on (H, Mo, and Zn)-ZSM5 zeolite under nonoxidizing conditions. The only hydrocarbon product was benzene, obtained over catalytic conversion of methane at high temperature (973 K). A carbenium ion mechanism of the activation of methane is suggested. In the case of H-ZSM5 a protonic site may act as a hydride acceptor, giving molecular hydrogen directly. Here the transition state involved in the dehydrogenation reaction of methane (eq 2) was also studied. An asymmetric exchange between the proton of the zeolite and CH_3 group (from CH_4) results in the elimination of an H_2 molecule. This reaction is of interest because it can be used as a model for C−H activation that leads to a carbenium ion from alkanes.

Additionally, from the calculated activation barriers and the vibrational, translational and rotational partition functions of the reactants and transition states, an analysis of the rate constants of reactions 1b and 2 can be made.

2. Method

2.1. Computational Details. All calculations in this work are based on density functional theory (DFT),[12] and for comparison, the semiempirical MNDO[13] method was used. The molecular system used in this paper consisted of a methane molecule and two different size tritetrahedral $H_3SiOHAl(OH)_2OSiH_3$ and $H_3SiOHAlH_2OSiH_3$ clusters that represent acidic zeolite. The peripheral bonds of the clusters, which are in reality connected to the zeolite framework, were saturated with H or OH. No constraint of symmetry has been used.

The density functional calculations reported in this work were done using the DGauss program, version 2.1, part of the UniChem package from Cray Research Inc.[14] The calculations were carried out on two different levels. The first is the local density approximation (LDA) using the exchange-correlation potential in the form given by Vosko, Wilk, and Nusair.[15] At the second level, nonlocal correlation and nonlocal exchange corrections due to Perdew[16] and Becke,[17] respectively, are added after the geometry optimization (NLDA) to the final total LDA energy. For some calculations, the NLDA correction is also included in a self-consistent manner (NLDA-SCF).

Molecular orbitals are expressed by linear combination of atomic Gaussian-type orbitals. The basis sets are of double-ζ quality and include polarization functions for all non-hydrogen atoms (DZPV).[18] The basis sets used were optimized for use in density functional calculations in order to minimize the basis set superposition error (BSSE), as has been demonstrated by Radzio et al.[19] in studies of the Cr_2 molecule. A second set of basis functions, the auxiliary basis set,[20] is used to expand the electron density in a set of single-particle Gaussian-type functions.

Total LDA energy gradients are computed analytically,[21] and calculations of geometry optimization to a minimum and saddle point (transition state, TS) are performed. In the last case (TS), the norm of the gradient is minimized and not the energy.[22] The frequencies are obtained by evaluating the matrix of the second derivatives by a finite difference scheme using the analytic first derivatives.[23] Unscaled frequencies have been used and zero-point energy (ZPE) corrections included.

2.2. Reaction Rate Constants. The reaction rate constants have been calculated using the transition state reaction rate theory, TST.[24] It is based on the application of statistical mechanics to reactants and activated complexes.

For the present case, bearing in mind that the cluster represents an "infinite" zeolitic surface, where the mass and the number of atoms go to infinity, the inclusion of a methane molecule does not affect the total (very large) mass of the system. This makes the rotational and translational partition functions for the transition state nearly the same as those for the cluster (HZ), resulting in them canceling each other. It is thus necessary to calculate only the ones which differ. The reaction rate constant (k) expressed in terms of "rate per acidic proton" for methane activation is then given by

$$k = (N_A V)\left(\frac{k_B T}{h}\right)\frac{q^{\ddagger}_{v(TS)}}{q_v q_r q_{t(CH_4)} q_{v(HZ)}} e^{-\frac{E_b}{k_B T}} \qquad (3)$$

where N_A, h, and k_B are Avogadro, Planck, and Boltzman's constants, respectively. V is the volume of the system, T is the temperature, and E_b is the activation barrier which already includes the ZPE corrections. For methane, the vibrational (q_v), rotational (q_r), and translational (q_t) partition functions need to be calculated, and for the TS and the cluster (HZ) only the vibrational partition function must be evaluated.

The natural logarithm of the reaction rate constant, ln k, can be approximated by a linear function of the reciprocal temperature $1/T$ according to the equation

$$\ln k = -\frac{E_{act}}{k_B T} + \ln A^{TST} \qquad (4)$$

where E_{act} is the Arrhenius activation energy and A^{TST} is the preexponential factor. The former is related to the change in activation entropy of the system on going from reactants to TS.

Finally, a comparison between the preexponent (A^{TST}) obtained with the transition state theory and the hard sphere preexponent (A^{HS}) which gives the number of collisions of a methane molecule approximated as a hard sphere can be done. The latter sets an upper limit for the first. The hard sphere preexponent is given by

$$A^{HS} = N_A \pi r^2 \left(\frac{8 k_B T}{\pi m}\right)^{1/2} \qquad (5)$$

where m is the mass of CH_4 and πr^2 is the collision cross section approximated by the size of the methane molecule. A small

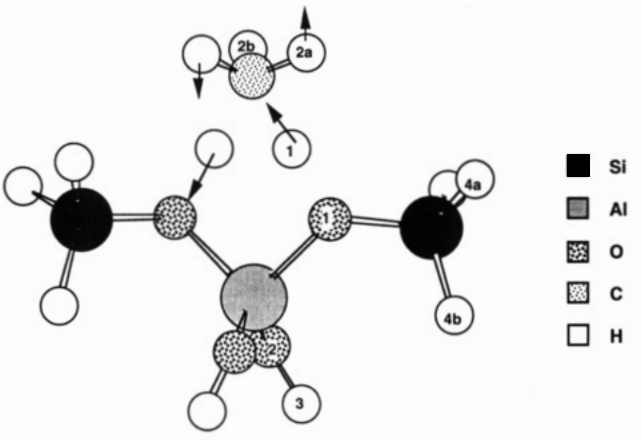

Figure 1. Reaction coordinate for the exchange process between methane and an acidic zeolite cluster. The arrows indicate the main components of the displacement vectors along the reaction coordinate. In this picture the TS-AlOH is represented. The TS-AlH is analogous, except for the OH's of aluminum, which are replaced by H's.

A^{TST}/A^{HS} ratio means a significant decrease in reaction entropy, due to loss in rotational or translational degrees of freedom.

3. Results

For easier reference, the two different clusters $H_3SiOHAl(OH)_2OSiH_3$ and $H_3SiOHAlH_2OSiH_3$ will be named clusters AlOH and AlH, respectively.

No important differences in energy or geometry have been found when nonlocal correction is included self-consistently (NLDA-SCF) instead of at the end of the geometry optimization to a minimum or saddle point (NLDA). Since NLDA-SCF considerably increases the calculation time, only the smaller AlH cluster has been studied using this method.

3.1. Hydrogen/Hydrogen Exchange. Figure 1 shows the calculated transition state and the corresponding reaction coordinate for the hydrogen exchange reaction. This TS has been obtained using NLDA included at the end of the calculation, and the AlOH cluster has been used. The reaction coordinate represents the symmetrical transfer of the proton of the zeolite to the methane molecule and the return of the hydrogen atom from the methane to the zeolite. In this process two oxygen atoms of the zeolite are involved, one as a proton acceptor (basic) and the other as a proton donor (acid). In the transition state both hydrogens are halfway between the carbon and oxygen atoms. Although no symmetry has been imposed, the structure obtained is approximately of C_s symmetry. The accuracy of the distances is within ±0.005 Å.

Table 1 shows the energetic and dynamic information obtained for the fragments (CH_4 and clusters) as well as for the TS's calculated for both reactions, hydrogen exchange and dehydrogenation. In Table 2 energy barriers (E_0) for both reactions are presented. Corrections for ZPE (E_b) are also shown in this table. As was already found by Fan et al.,[25] for reactions involving transfer of protons, LDA without nonlocal corrections gives too small barriers. The values found for clusters AlH and AlOH are 50 and 41 kJ/mol (including ZPE), respectively. This shows that the inclusion of nonlocal corrections is very important in this kind of reaction. The activation barriers obtained from MNDO calculations are much too high, 384 and 373 kJ/mol, respectively, for AlOH and AlH clusters (including ZPE). This shows that this method can not be recommended for the calculation of TS energies. However, although the energies are not correct, it is a very useful method (cheap in terms of computer time) to get a first estimate of the geometry of the transition state. From Table 2 it can be seen that the terminal group on aluminum does not affect the resultant activation barrier. It is found to be 131 kJ/mol for AlH and 132 kJ/mol for the AlOH cluster. If NLDA-SCF is included the barrier increases to 137 kJ/mol (for the AlH cluster). These results are lower than previous results for an equivalent cluster, 150 ± 20 kJ/mol using SDCI/6−31G**,[6] and for a smaller cluster, 167 kJ/mol (or 155 kJ/mol if ZPE is included) using MP2/6−31++G**.[8] If corrections for ZPE are accounted for, the barriers decrease by 10−12 kJ/mol. The ZPE-corrected activation barriers that follow from the present study are around 120−125 kJ/mol, depending on cluster size and rigor of calculation. According to Kramer's estimate, the effective reaction barrier for the methane deutero exchange is 122 kJ/mol. The results obtained in this paper (120−125 kJ/mol) are in very good agreement with this value.

The distances can be seen in Table 3. Between oxygen (O1) and the proton (H1), the computed distance is 1.31 Å, and the carbon−proton distance is found to be 1.34 Å for both clusters, AlH and AlOH. In the NLDA-SCF calculations, these distances are slightly larger, 1.33 (O1−H1) and 1.35 Å (C−H1). These distances are found to be quite similar. This is different from the results obtained by Kramer et al.[6] and Evleth et al.[8] Kramer et al. obtained C−H (1.39 Å) 0.19 Å larger than O−H (1.20 Å), and Evleth obtained also a much larger difference (0.34 Å) for the same distances (1.16 and 1.50 Å). Repeating the DFT NLDA calculation for TS-AlH using the 3−21G and 6−31G* basis set of Pople, the difference obtained for these two distances is slightly larger (0.04 Å) for 6−31G* and considerably larger (0.12 Å) for 3−21G. In the MNDO calculations the difference of C−H and O−H distances is on the order of 0.69 Å. These differences imply that both basis set and methodology (DFT or Hartree−Fock) used can significantly change the predicted atomic distances. Considering that the calculated activation barriers are in good agreement with experiment, it is assumed that the DFT geometries obtained are also accurate.

Table 4 gives the computed Mulliken charges. The behavior of Mulliken charges for both clusters, AlH and AlOH, is similar except for the aluminum atom. As is to be expected, the positive charge of Al terminated by two hydroxyl groups (cluster AlOH) is larger than that of the AlH cluster, in which the aluminum atom is terminated by two single hydrogen atoms. There are two possible explanations: the presence of the two oxygen atoms, which are more electronegative than the hydrogen atoms, or an artifact of the Mulliken charges calculation, which distributes the total charge among the orbitals. Since the oxygen atoms have a bigger number of orbitals, the OH group can receive a bigger charge than single hydrogen atoms, and the aluminum atom becomes more positive in the first case than in the latter. When an analysis of the geometry, motion, and charge of the atoms that actually participate in the reaction coordinate in the transition state is done, one can see that no significant difference is found. This shows that, despite the fact that the AlOH cluster seems closer to the real zeolite than the AlH cluster (due to the presence of the hydroxyl rather than hydrogen in the terminal position of the aluminum atom), both clusters seem to be suitable for representing the zeolite.

Contrary to Evleth's results, the CH_3 group is positively charged (+0.12) for the TS's involving NLDA corrections (AlOH and AlH clusters). When the same analysis is made for the charges obtained by NLDA-SCF calculation, it is possible to see that the CH_3 group is found to be slightly negatively charged (-0.08) but can hardly be characterized as an anion. Taking into consideration the fact that the NLDA-SCF is a better correction than the simple NLDA, the first case is to be considered more precise than the last. The charge for the $CH_5^{\delta+}$

TABLE 1: Energies (hartree) and Imaginary Frequencies (IF, in cm^{-1}) of the Fragments (CH_4 and Clusters) and the TS's of the Reactions of Hydrogen Exchange and Dehydrogenation of Methane

	NLDA-SCF	NLDA	LDA	MNDO (eV)
		Fragments		
cluster AlOH		−1128.044 525	−1122.416 807	−1647.704 93
cluster AlH	−977.436 479	−977.424 512	−972.842 125	−999.653 10
CH_4	−40.524 428	−40.522 376	−40.110 503	−185.091 37
		Hydrogen Exchange		
TS-AlOH		−1168.516 774	−1162.507 645	−1828.734 83
IF-AlOH		−1389.4		−758.5
TS-AlH	−1017.908 567	−1017.897 188	−1012.929 680	−1180.808 60
IF-AlH	−1609.7	−1432.2		−789.4
		Dehydrogenation		
TS-AlOH		−1168.431 632	−1162.417 207	−1826.811 20
IF-AlOH		−1074.0		−1545.7, −53.1[a]
TS-AlH	−1017.826 086	−1017.812 542	−1012.837 890	−1178.940 16
IF-AlH	−1015.7	−1106.8		−1547.6

[a] For this TS, a second imaginary frequency was impossible to remove. This frequency is related to the H's bonded to Si atoms and to the OH's bonded to Al, not influencing the reaction coordinate.

TABLE 2: Electronic Activation Barrier (E_0), Activation Barrier Including ZPE (E_b), Arrhenius Activation Energy (E_{act}, in kJ/mol), and Arrhenius Preexponent (A^{TST}, in $m^3\ mol^{-1}\ s^{-1}$) for Both Reactions, Hydrogen Exchange and Dehydrogenation of Methane

	hydrogen exchange				dehydrogenation			
	NLDA-SCF	NLDA	LDA	MNDO	NLDA-SCF	NLDA	LDA	MNDO
				TS-AlOH				
E_0		131.6	51.6	391.9		355.1	289.1	577.5
E_b		121.2	41.2	383.5		347.9	281.9	568.4
E_{act}		126.5				351.6		
A^{TST}		1.10×10^5				3.04×10^3		
				TS-AlH				
E_0	137.4	130.5	60.2	379.7	354.0	352.7	301.2	560.0
E_b	125.1	120.3	50.0	373.4	343.0	343.7	292.2	554.1
E_{act}	129.5	125.0			348.5	348.4		
A^{TST}	5.09×10^4	3.99×10^4			2.45×10^4	1.50×10^4		

TABLE 3: Geometry for the TS of the Hydrogen Exchange Reaction (Distances in Å and Angles in deg)

	AlH		AlOH		
	NLDA-SCF	NLDA	NLDA	MNDO	ref[8]
O1−H1	1.332	1.308	1.310	1.026	1.156[a]
C−H1	1.346	1.339	1.337	1.718	1.496[b]
C−H2a,a′	1.103	1.106	1.105	1.103	1.088
C−H2b	1.109	1.111	1.111	1.102	1.090
Si−O1	1.690	1.675	1.674	1.696	
O1−A1	1.883	1.852	1.818	1.803	1.860
Al−O2[c]	1.608	1.606	1.726	1.699	1.583; 1.594
O2−H3			0.974	0.930	
Si−H4a,a′	1.500	1.502	1.503	1.375	
Si−H4b	1.498	1.501	1.501	1.376	
SiO1Al	126.5	125.62	125.31	134.4	
O1AlO1′	90.9	91.4	92.3	98.1	

[a] Distance obtained by ref 6, 1.201 Å. [b] Distance obtained by ref 6, 1.391 Å. [c] For AlH cluster, instead of O_2 read H.

TABLE 4: Mulliken Charges for the TS of the Hydrogen Exchange Reaction

	AlH		AlOH		
	NLDA-SCF	NLDA	NLDA	MNDO	ref 8
Si	0.411	0.283	0.301	1.632	
Al	0.478	0.323	0.735	1.010	0.64
O1	−0.756	−0.684	−0.661	−0.588	−0.63
O2[a]	−0.081	−0.039	−0.711	−0.588	−0.20; −0.22
C	−0.819	−0.688	−0.689	−0.560	−0.77
H1	0.294	0.286	0.287	0.306	0.26
H2a,a′	0.245	0.266	0.267	−0.500	0.16
H2b	0.253	0.277	0.278	−0.500	0.16
H3			0.430	0.182	
H4a,a′	−0.030	0.005[a]	0.007[b]	−0.364	
H4b	−0.014	0.017	0.010	−0.367	

[a] For AlH cluster, instead of O_2 read H. [b] One of the hydrogens (H4a) bonded to Si has charge −0.006.

group is +0.51 for the NLDA-SCF calculation and +0.70 (AlOH) and +0.69 (AlH) for NLDA. Evleth obtained a charge of +0.23, which is considerably smaller. In essence, these results seem to agree, keeping in mind the severe arbitrariness of the Mulliken charge analysis. The Mulliken charges obtained with the MNDO method are different from those obtained in DFT and HF calculations. With this method, the $CH_5^{\delta+}$ group is negatively charged, which is not correct.

Table 5 shows the obtained rate constants for different temperatures. The rate constants increase when hydride termination is changed to hydroxyl termination ($k_{(AlH)} < k_{(AlOH)}$) and decrease with increasing rigor of the calculation ($k_{(NLDA-SCF)} < k_{(NLDA)}$). The Arrhenius plot (ln k versus $1000/T$) is shown in Figure 2. From a linear fit of the curves, the activation energy of Arrhenius (E_{act}) as well as the preexponents (A^{TST}) can be calculated. The values can be seen in Table 2. The activation barriers (E_0 and E_b) and activation energy (E_{act}) differ by a few kilojoules per mole. In general, for this reaction (hydrogen exchange) the inclusion of ZPE corrections decreases the activation barriers by 10−12 kJ/mol. The Arrhenius activation energy lies between E_0 and E_b. The preexponent ratio (A^{TST}/A^{HS}) for various temperatures is shown in Table 6. The ratio obtained is quite small (10^{-3}−10^{-4}) which shows a considerable decrease in the entropy of the system due to loss of rotational and translational degrees of freedom. This suggests that the transition state obtained is tight, which means that in the transition state the methane molecule is rigidly attached to the zeolitic cluster. It is a reflection of the small distances

TABLE 5: Rate Constants (k, in $m^3\ mol^{-1}\ s^{-1}$) for Different Temperatures (T, in K)

	hydrogen exchange			dehydrogenation		
	AlH		AlOH	AlH		AlOH
T	NLDA-SCF	NLDA	NLDA	NLDA-SCF	NLDA	NLDA
273	1.30×10^{-20}	7.32×10^{-20}	1.05×10^{-19}	8.79×10^{-63}	5.55×10^{-63}	2.74×10^{-64}
473	1.85×10^{-10}	4.46×10^{-10}	8.53×10^{-10}	5.65×10^{-35}	3.60×10^{-35}	3.27×10^{-36}
673	3.38×10^{-06}	5.79×10^{-06}	1.24×10^{-05}	1.59×10^{-23}	9.98×10^{-24}	1.15×10^{-24}
873	8.67×10^{-04}	1.24×10^{-03}	2.83×10^{-03}	3.26×10^{-17}	2.02×10^{-17}	2.64×10^{-18}
1073	3.30×10^{-02}	4.19×10^{-02}	9.97×10^{-02}	3.49×10^{-13}	2.15×10^{-13}	3.03×10^{-14}

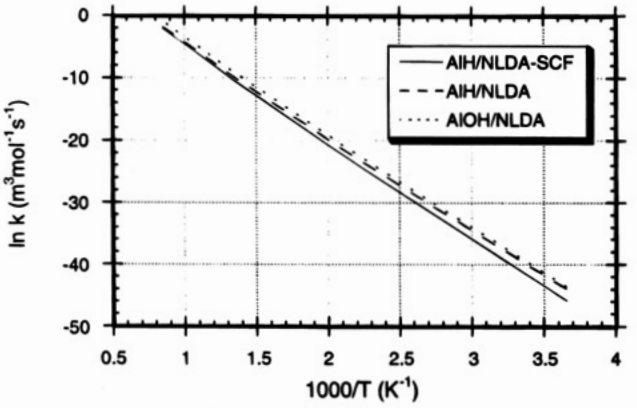

Figure 2. Arrhenius plot: temperature (T) dependence of the natural logarithm of the rate constants, ln(k), for the hydrogen exchange reaction between methane and an acidic zeolite.

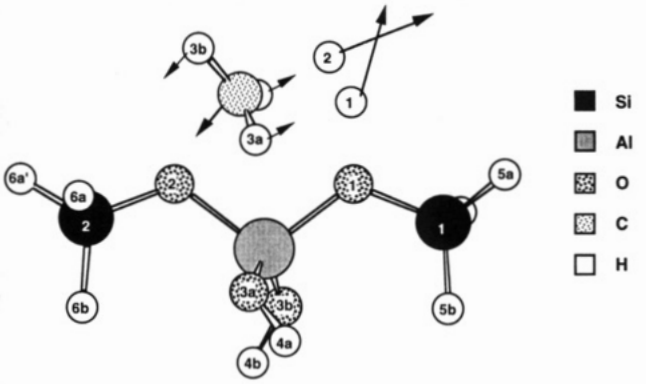

Figure 3. Reaction coordinate for the dehydrogenation process between methane and an acidic zeolite cluster. The arrows indicate the main components of the displacement vectors along the reaction coordinate. In this picture the TS-AlOH is represented. The TS-AlH is analogous, except for the OH's of aluminum, which are replaced by H's.

between the protons around the carbon atom and oxygen atoms of the cluster.

3.2. Dehydrogenation. In the Figure 3 the calculated transition state and corresponding reaction coordinate for the dehydrogenation reaction are represented. The reaction coordinate illustrates the asymmetrical movement of the proton (H1), with one hydrogen atom from the methane, into the direction of formation of a H_2 molecule. The carbon atom tends to bind to the basic oxygen atom (O2) of the zeolite cluster, resulting in a CH_3−zeolite complex. The structure obtained has approximately the C_s symmetry although no symmetry has been imposed.

The energies and imaginary frequencies for the calculated transition states can be found in Table 1, and the activation barriers, in Table 2. Assuming that, just as for hydrogen exchange, NLDA gives better results, we find that the LDA and MNDO results give too low and too high activation barriers, 282 and 568 kJ/mol, respectively (both using the AlOH cluster and including ZPE). The barriers obtained with NLDA and NLDA-SCF for the AlH cluster are respectively 344 and 343 kJ/mol, and for the AlOH cluster it is 348 kJ/mol (ZPE included in all cases). These numbers are around 220 kJ/mol higher than the ones obtained for hydrogen exchange. This confirms the fact that the dehydrogenation reaction of methane catalyzed by an acidic zeolite is much more difficult than its hydrogen exchange reaction.

No experimental activation barrier for the methane dehydrogenation is available. Iglesia et al.[26] found an activation barrier for the dehydrocyclization of n-heptane of 215 kJ/mol. Hydrogen exchange between undeuterated and perdeuterated light alkanes (CD_4−C_3H_8) and (C_3D_8−C_3H_8) over (H, Ga, and Zn)-ZSM5 occurs at 773 K, according to studies from Iglesia et al.[27] They found that H-ZSM5 also activates the C−H bond in methane but much more slowly than it activates the weaker and more reactive propane, with the rate of C−H activation for methane being 20 times slower than that for propane (for the reactant mixture used). Not only is the C−H bond strength of importance to the heterolytic C−H bond dissociation but the stabilities of the carbocation and of its hydridic H atom counterpart are also important. Stefanadis et al.[28] found an effective activation energy for isobutane catalyzed by a H-ZSM5 zeolite of 57 kcal/mol (238 kJ/mol). The important difference between isobutane and methane dehydrogenation is that in the former case a tertiary carbenium is generated. Calculations using the DFT/NLDA method showed the following difference in the stability of carbenium ions with respect to the neutral molecules (in kJ/mol):

$$H_3C^+ \overset{199}{<} CH_3H_2C^+ \overset{96}{<} (CH_3)_2HC^+ \overset{66}{<} (CH_3)_3C^+$$

This explains why the activation energy for the dehydrogenation of methane is much higher than that obtained experimentally by Stefanadis et al.[28] for the dehydrogenation of isobutane, which proceeds via a tertiary carbocation.

TABLE 6: Preexponent Ratio (A^{TST}/A^{HS}) for Different Temperatures (T, in K)

	hydrogen exchange			dehydrogenation		
	AlH		AlOH	AlH		AlOH
T	NLDA-SCF	NLDA	NLDA	NLDA-SCF	NLDA	NLDA
273	6.70×10^{-4}	5.11×10^{-4}	1.44×10^{-3}	3.22×10^{-4}	1.97×10^{-4}	4.00×10^{-5}
473	5.09×10^{-4}	3.88×10^{-4}	1.10×10^{-3}	2.45×10^{-4}	1.50×10^{-4}	3.04×10^{-5}
673	4.27×10^{-4}	3.25×10^{-4}	9.20×10^{-4}	2.05×10^{-4}	1.26×10^{-4}	2.55×10^{-5}
873	3.75×10^{-4}	2.86×10^{-4}	8.08×10^{-4}	1.80×10^{-4}	1.10×10^{-4}	2.24×10^{-5}
1073	3.38×10^{-4}	2.58×10^{-4}	7.28×10^{-4}	1.62×10^{-4}	9.97×10^{-5}	2.02×10^{-5}

TABLE 7: Geometry of the TS for the Dehydrogenation Reaction (Distances in Å and Angles in deg)

	AlH		AlOH	
	NLDA-SCF	NLDA	NLDA	MNDO
O1−H1	1.590	1.492	1.524	0.996
H1−H2	0.869	0.915	0.908	1.386
C−O2	2.118	1.978	1.990	1.510
C−H2	1.666	1.662	1.643	1.559
C−H3a,a′	1.084	1.090	1.090	1.131
C−H3b	1.102	1.103	1.104	1.133
Si−O1	1.687	1.672	1.673	1.701
Si−O2	1.683	1.676	1.673	1.702
O1−Al	1.899	1.869	1.833	1.815
O2−Al	1.883	1.863	1.833	1.812
Al−O3a,b[a]	1.610	1.610	1.729	1.703
O3a,b−H4a,b			0.974	0.930
Si−H5a,a′	1.502	1.502	1.502	1.375
Si−H5b	1.501	1.504	1.503	1.376
Si1O1Al	122.3	120.53	120.30	132.4
Si2O2Al	122.2	118.70	120.41	127.2
O1AlO2	106.9	106.73	108.34	108.0

For a first-order reaction, the effective activation energy equals the activation barrier minus the heat of adsorption. The adsorption energy for *n*-butane on different zeolites[29] is around 41 kJ/mol. The difference between the adsorption energy of *n*-butane and isobutane in (Na and H)-X zeolite[30] is 1 kJ/mol higher for isobutane. From this one obtains an activation barrier for the dehydrogenation of isobutane around 280 kJ/mol. According to the calculations obtained with DFT, carbenium ion (H_3C^+) is 361 kJ/mol less stable than $(CH_3)_3C^+$. However comparing the activation barriers of methane (343 kJ/mol) and isobutane (280 kJ/mol) dehydrogenation, one sees that the difference is much smaller (63 kJ/mol). This is due to charge stabilization of the carbenium ion by the zeolite converting the intermediates into a transition state.

The distances and some angles between atoms can be seen in Table 7. The distance between O1 and H1 in the TS tends to increase with increasing level of calculation and cluster size, the latter having a smaller effect than the former. For NLDA-SCF this distance is 1.59 Å, and for NLDA it is 1.49 Å, both referring to the AlH cluster. For the AlOH cluster, this distance is 1.52 Å. An analogous result is found for the (C−O2) distance, 2.12 Å for AlH at the NLDA-SCF level. For NLDA, the difference is smaller (1.99 Å for AlOH and 1.98 Å for AlH). As a consequence, the distance between the hydrogen atoms 1 and 2 tends to decrease with increasing level of calculation and cluster size. In the AlH cluster for NLDA-SCF, where it has its smallest value, 0.87 Å, it is still clearly larger than for the H_2 molecule in the gas phase, 0.746 Å.[31]

Mulliken charges are presented in Table 8. There one can see that the CH_3 group now has a positive charge in all different calculated TS's. Clearly the transition state corresponds to the generation of an almost neutral hydrogen atom from the zeolite that reacts with $H^{\delta+}$ from methane to form the H_2 molecule. The positively charged CH_3^+ group (a carbenium ion like) becomes stabilized by the zeolite oxygen atom.

In Table 5 are collected the obtained rate constants for different temperatures. Contrary to hydrogen exchange, the rate constants for the dehydrogenation reaction decrease when hydride is replaced by hydroxyls ($k_{(AlH)} > k_{(AlOH)}$) and increase with increasing rigor of calculation ($k_{(NLDA-SCF)} > k_{(NLDA)}$). The rates are much smaller than those obtained for the hydrogen/hydrogen exchange reaction. This is because of a much larger activation barrier for the dehydrogenation reaction. The Arrhenius plot is shown in Figure 4. A linear fit of the curves gives the activation energies of Arrhenius (E_{act}) and the preexponents (A^{TST}) which can be seen in Table 2. Just as for the hydrogen/hydrogen exchange reaction, the activation barriers E_0 and E_b and activation energy E_{act} differ by several kilojoules per mole. Inclusion of ZPE corrections decreases the activation barriers by 8−11 kJ/mol. The preexponent ratio (A^{TST}/A^{HS}) according to temperature is shown in Table 6. The ratio obtained is rather small (10^{-4} to 10^{-5}). This again shows a considerable decrease in the entropy of the system, due to loss of rotational and translational degrees of freedom. This suggests that, in the obtained transition state for the dehydrogenation reaction, the methane molecule is more strongly attached to the zeolite cluster than in the case of hydrogen exchange. Although the distance between the carbon atom and the zeolitic oxygen is quite large, the strong ionic interaction between the CH_3^+ group and the oxygen atom makes the methane molecule firmly attached to the zeolite.

4. Conclusions

The reactions of hydrogen exchange and dehydrogenation of methane catalyzed by an acidic zeolite have been studied utilizing DFT. Additionally, the reaction rate constants have been calculated by means of the transition state reaction rate theory. The activation barrier for the hydrogen exchange reaction (125 kJ/mol) is in very good agreement with an earlier estimate[6]. The activation barrier obtained for the dehydrogenation reaction is about three times larger than that obtained for the hydrogen exchange reaction (343 kJ/mol).

TABLE 8: Mulliken Charges for the TS of the Dehydrogenation Reaction of Methane

	AlH		AlOH	
	NLDA-SCF	NLDA	NLDA	MNDO
Si1	0.413	0.289	0.313	1.635
Si2	0.409	0.270	0.296	1.637
Al	0.404	0.229	0.668	1.024
O1	−0.738	−0.674	−0.663	−0.556
O2	−0.638	−0.569	−0.585	−0.624
O3a,b[a]	−0.072; −0.074	−0.024; −0.022	−0.727; −0.720	−0.592
C	−0.612	−0.702	−0.707	0.497
H1	0.165	0.160	0.169	0.309
H2	0.035	0.052	0.062	−0.659
H3a,a′	0.333; 0.326	0.343; 0.335	0.348	−0.070; −0.108
H3b	0.288	0.310	0.312	−0.108
H4a,b			0.435; 0.438	0.181
H5a,a′	−0.042; −0.031	−0.005; 0.005	−0.014; 0.013	−0.363
H5b	−0.024	0.009	0.001	−0.363
H6a,a′	−0.028; −0.048	−0.002; 0.007	−0.001; 0.002	−0.367
H6b	−0.021	0.016	0.012	−0.370

[a] For AlH cluster, instead of O_3 read H.

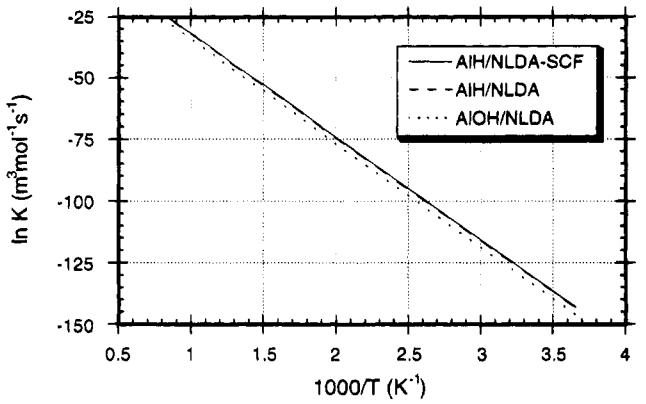

Figure 4. Arrhenius plot: temperature (T) dependence of the natural logarithm of the rate constants, $\ln(k)$, for the dehydrogenation reaction of methane over an acidic zeolite.

The reaction of hydrogen/hydrogen exchange of methane catalyzed by an acidic zeolite proceeds via a transition state that is considerably different from that for the acid-catalyzed dehydrogenation of methane. The transition state for hydrogen exchange has the characteristics of a carbonium ion that is stabilized by the negatively charged lattice oxygen atoms. The transition state for the dehydrogenation reaction has a local coordination around the carbon atom which is more carbenium like. This transition state is stabilized by a direct interaction of the carbon atom with a lattice oxygen atom and the proton involved in the hydrogen molecule formation.

The rate constants obtained for the dehydrogenation reaction are much smaller than those for hydrogen exchange due to a much higher activation barrier for the former. Also, the rates for hydrogen exchange show an opposite behavior concerning rigor of calculation and the kind of terminal group on the aluminum atom of the cluster than that for the dehydrogenation reaction. The preexponent ratio seems to be more sensible with respect to the kind of terminal group on the aluminum atom for both reactions. There is a considerable loss in rotational and translational entropy comparing the transition state and reactants in the gas phase for both reactions. According to the preexponent ratio, methane is more strongly attached to the zeolite in the transition state for the dehydrogenation reaction than for hydrogen exchange.

It is also concluded that the DFT method including nonlocal corrections demonstrated considerable promise as a practical tool in kinetic studies in the zeolite field. For the present reactions, the LDA method gives a barrier that is too low and MNDO gives a barrier that is much too high. The cluster size does not affect the motion or geometry of the atoms involved in the reaction coordinate but seems to be more important when referring the kinetics of the reactions. The inclusion of nonlocal correction self-consistently is assumed to give more accurate results (activation barriers, charges, and geometries) due to better correction.

Acknowledgment. S.R.B. thanks the National Council of Scientific and Technologic Development (CNPq, Brazil) for a scholarship. M.A.C.N. thanks CNPq and Finep for financial support. Computational resources were supplied by the national computing facilities foundation (NCF, The Netherlands) under Project SC-183.

References and Notes

(1) (a) Kerr, G. T. *Sci. Am.* **1989**, *261*, 100. (b) Vaughan, D. E. W. *Chem. Eng. Prog.* **1988**, *84*, 25.
(2) *Introduction to zeolite science and practice*; van Bekkum, H., Flanigen, E. M., Jansen, J. C., Eds.; Studies in Surface Science and Catalysis 58; Elsevier: Amsterdam, The Netherlands, 1991; Chapter 15.
(3) *Introduction to zeolite science and practice*; van Bekkum, H., Flanigen, E. M., Jansen, J. C., Eds.; Studies in Surface Science and Catalysis 58; Elsevier: Amsterdam, The Netherlands, 1991; Chapter 12.
(4) Iglesia, E.; Baumgarter, J. E. *Catal. Lett.* **1993**, *21*, 55.
(5) Kramer, G. J.; van Santen, R. A. *J. Am. Chem. Soc.* **1993**, 115, 2887.
(6) Kramer, G. J.; van Santen, R. A. Emeis, C. A.; Novak, A. K. *Nature* **1993**, *363*, 529.
(7) Olah, G. A.; Prakash, G. K.; Williams, R. E.; Field, L. D.; Wade, K. *Hypercarbon Chemistry*; John Wiley & Sons: New York, 1987.
(8) Evleth, E. M.; Kassab, E.; Sierra, L. R. *J. Phys. Chem.* **1994**, *98*, 1421.
(9) (a) Mota, J. A.; Martins, R. L. *J. Chem. Soc., Chem. Commun.* **1991**, 171. (b) Mota, C. J. A.; Nogueira, L.; Cover, W. B. *J. Am. Chem. Soc.* **1992**, *114*, 1121.
(10) Burghgraef, H.; Jansen, A. P. J.; van Santen, R. A. *J. Chem. Phys.* **1993**, *177*, 407.
(11) Wang, L.; Tao, L.; Xie, M.; Xu, G.; Huang, J.; Xu, Y. *Catal Lett.* **1993**, *21*, 35.
(12) (a) Hohenberg, P.; Kohn, W. *Phys. Rev. B* **1964**, *136*, 864. (b) Kohn, W.; Sham, L. J. *Phys. Rev. A* **1965**, *140*, 1133.
(13) Dewar, M. J. S.; Thiel, W. *J. Am. Chem. Soc.* **1977**, *99*, 4899.
(14) Andzelm, J.; Wimmer, E. *J. Chem. Phys.* **1992**, *96*, 1280.
(15) Vosko, S. H.; Wilk, L.; Nusair, M. *Can. J. Phys.* **1980**, *58*, 1200.
(16) Perdew, J. P. *Phys. Rev. B* **1986**, *33*, 8822.
(17) Becke, A. D. *Phys. Rev. A* **1988**, *33*, 3098.
(18) Godbout, N.; Andzelm, J.; Wimmer, E.; Salahub, D. R. *Can. J. Chem.* **1992**, *70*, 560.
(19) Radzio, E.; Andzelm, J.; Salahub, D. R. *J. Comput. Chem.* **1985**, *6*, 553.
(20) Andzelm, J.; Russo, N.; Salahub, D. R. *Chem. Phys. Lett.* **1987**, *142*, 169.
(21) (a) Shlegel, H. B. *Ab initio methods in Quantun Chemistry*; Lawley, K. P., Ed.; John Wiley & Sons: New York, 1987. (b) Head, J. D.; Zerner, M. C. *Ad. Quantum Chem.* **1989**, *20*, 239.
(22) McIver, J. W.; Kormornicki, A. *Chem. Phys. Lett.* **1971**, *10*, 303.
(23) Wilson, E. B.; Decius, J. C.; Cross, P. C. *Molecular Vibrations*; Mc Graw-Hill: New York, 1955.
(24) Moore, J. W.; Pearson, R. G. *Kinetics and Mechanisms*; John Wiley & Sons: New York, 198. (b) Frost, A. A.; Pearson, R. G. *Kinetics and Mechanisms*; John Wiley & Sons: New York, 1961.
(25) Fan, L.; Ziegler, T. *J. Am. Chem. Soc.* **1992**, *114*, 10890.
(26) Iglesia, E.; Baumgartner, J. E.; Price, G. L. *J. Catal.* **1992**, *134*, 549.
(27) Iglesia, E.; Baumgartner, J. E. *Catal. Lett.* **1993**, *21*, 55.
(28) Stefanadis, C.; Gates, B. C.; Hang, W. O. *J. Mol. Catal.* **1991**, *67*, 363.
(29) Stach, H.; Fiedler, K.; Jänchen, J. *Pure Appl. Chem.* **1993**, *65*, 2193.
(30) Atkinson, D.; Curthoys, G. *J. Chem. Soc., Faraday Trans. I* **1981**, *77*, 897.
(31) Lide, D. R., Ed. *Handbook of Chemistry and Physics*, 71st ed.; CRC Press: Boca Raton, FL, 1990.